

AMCoR

Asahikawa Medical College Repository <http://amcor.asahikawa-med.ac.jp/>

Skeletal Radiology (2009) 38(2):131–139.

Three-dimensional computed tomography analysis of non-osteoarthritic adult acetabular dysplasia.

Ito H, Matsuno T, Hirayama T, Tanino H, Yamanaka Y,
Minami A.

Three-dimensional computed tomography analysis of non-osteoarthritic adult acetabular dysplasia

Hiroshi Ito · Takeo Matsuno · Teruhisa Hirayama · Hiromasa Tanino · Yasuhiro Yamanaka ·
Akio Minami

H. Ito · T. Matsuno · T. Hirayama · H. Tanino · Y. Yamanaka

Department of Orthopaedic Surgery, Asahikawa Medical College

Midorigaoka Higashi 2-1-1-1, Asahikawa, 078-8510, Japan

A. Minami

Department of Orthopaedic Surgery, Hokkaido University School of Medicine

Kita-ku Kita-15 Nishi-7, Sapporo, 060-8638, Japan

Corresponding Author: Hiroshi Ito

Department of Orthopaedic Surgery, Asahikawa Medical College

Midorigaoka Higashi 2-1-1-1, Asahikawa, 078-8510, Japan

Phone #81-166-68-2511 Fax #81-166-68-2519

E-mail itohiro@asahikawa-med.ac.jp

**Three-dimensional computed tomography analysis of non-osteoarthritic adult
acetabular dysplasia**

Abstract

Objective Little data exists on the original morphology of acetabular dysplasia obtained from patients without radiographic advanced osteoarthritic changes. The aim of this study was to investigate the distribution and degree of acetabular dysplasia in a large number of patients showing no advanced degenerative changes using three-dimensional computed tomography (3DCT).

Materials and methods Eighty-four dysplastic hips in 55 consecutive patients were studied. All 84 hips were in pre- or early osteoarthritis without radiographic evidence of joint space narrowing, formation of osteophytes or cysts, or deformity of femoral heads. The mean age at the time of CT scan was 35 years (range 15–64 years). 3D images were reconstructed and analyzed using recent computer imaging software (INTAGE Realia and Volume Player). Deficiency types and degrees of acetabular dysplasia were precisely evaluated using these computer software.

Results The average Harris hip score at CT scans was 82 points. Twenty-two hips (26%) were classified as anterior deficiency, 17 hips (20%) as posterior deficiency, and 45 hips (54%) as lateral deficiency. No significant difference was found in the Harris hip score among these groups. The analysis of various measurements indicated wide variations. There was a significant correlation between the Harris hip score and the acetabular coverage ($p < 0.001$).

Conclusion Our results indicated wide variety of deficiency type and degree of acetabular dysplasia. Hips with greater acetabular coverage tended to have a higher Harris hip score.

Key words Hip dysplasia, Computed tomography, Congenital hip dislocation, Hip osteoarthritis

Introduction

Early secondary osteoarthritis of the hip often develops in young adults who have a dysplastic acetabulum [1-7]. Wiberg described the development of osteoarthritic changes in young adults who had a dysplastic hip with $<20^\circ$ of the centre-edge (CE) angle on antero-posterior radiographs [6, 7]. Murphy et al. [2] reported that no patient in whom the hip functioned well until the age of 65 years had had $<16^\circ$ of the CE angle. Malvitz and Weinstein [1] indicated that the function of the hip in patients with developmental dysplasia might be well for many years, however, it tended to deteriorate after those periods of time. Increased joint contact pressures which were estimated from radiographs at the time of maturity of patients with developmental dysplasia have been reported to correlate with unsatisfactory clinical and radiographic outcome [8, 9]. When planning hip surgery for patients with developmental dysplasia, accurate assessment of the degree of subluxation, dislocation or acetabular dysplasia is essential [2, 10-22].

Information about lateral coverage of the femoral head has been obtained from conventional antero-posterior radiographs by measuring the CE angle [6, 7], and about anterolateral coverage from false-profile lateral radiographs by measuring the anterior centre-edge (ACE) angle [23]. Plain radiographs allow a diagnosis of dysplasia to be made [1-9, 23-28], however, these two-dimensional (2D) images lack three-dimensional (3D) information and accurate quantification of the degree and location is difficult.

Several studies using 3D computed tomography (CT) demonstrated its efficacy for precise evaluation of various acetabular deficiencies depending on patients before pelvic osteotomies [10, 11, 13, 17, 19, 21]. Adult hip dysplasia has been classified as anterior, posterior, or global deficiency in previous studies [11, 18-20, 24, 25, 28, 29], however, the

numbers of evaluated patients in these studies were relatively small and it is not clear whether each deficiency has various degrees of dysplasia. Furthermore, the patients reported in previous studies included those demonstrating radiographic advanced degenerative changes such as joint space narrowing, deformity of the femoral head, and formation of osteophytes or cysts [14, 16, 17, 19, 25]. Little data exists on the original morphology of acetabular dysplasia obtained from patients without these advanced changes to eliminate effects by osteoarthritis [6, 25].

The recent development and prevalence of computer imaging software have enabled the description of 3D morphology [11, 17, 19, 22]. Imaging data can be transferred from 3DCT to personal computers by electronic media. The 3D reconstruction can be directly made on personal computers using recent software and media, which facilitates precise evaluation of the severity of acetabular dysplasia.

In the present study, we ascertained whether: (1) acetabular dysplasia has various deficiency types and degrees depending on patients rather than a specific type having specific severity; (2) 3DCT and recent imaging software are useful to analyze individual characteristics of acetabular dysplasia; and (3) 3D image reconstruction can be easily performed using recent imaging software installed on a personal laptop computer.

Materials and Methods

This study was approved by the local institutional review board. All investigations were conducted in conformity with ethical principles of research. Informed consent for this study was obtained from all patients.

From February 2000, 3DCT scans were performed for consecutive adult patients with

hip dysplasia who were admitted to our hospital for hip surgery or precise evaluations of dysplasia. Criteria for enrollment in the study were as follows: radiographic evidence of acetabular dysplasia with $<20^\circ$ of the CE angle of Wiberg on AP radiographs [7], Crowe type-I subluxation [26], no radiographic evidence of joint space narrowing, formation of osteophytes or cysts, or deformity of femoral heads in order to eliminate secondary changes by osteoarthritic involvement; and no previous operation on the acetabulum. In Crowe type-I developmental dysplasia of the hip, the vertical subluxation of the hip (measured from the inferior margin of the tear drop to the head-neck junction) is $<50\%$ of the diameter of the femoral head (or $<10\%$ of the height of the pelvis). Hips without any degenerative changes such as joint space narrowing, formation of osteophytes or cysts were defined as pre-osteoarthritic stage. Hips showing only slight sclerotic changes without other radiographic evidence of osteoarthritis were considered to be acceptable for enrollment and were defined as having early osteoarthritis. Patients in whom dysplasia might have been affected by neurological illness or Legg-Calvé-Perthes disease were excluded. Fourteen patients with bilateral involvement had unilateral pre- or early osteoarthritis and contralateral advanced osteoarthritis. These 14 hips with pre- or early osteoarthritis fulfilled the criteria and were included in this study. In the 14 contralateral hips with advanced osteoarthritis, five hips had undergone total hip arthroplasty and two hips had undergone Chiari pelvic osteotomy at the time of CT examination. Thirty-two patients had bilateral involvement and both hips were in pre- or early osteoarthritis. Of these, three hips had undergone unilateral periacetabular osteotomy and were excluded from the analysis. Nine patients who had unilateral involvement of pre- or early osteoarthritis were included. Therefore, 84 dysplastic hips in 55 adult patients (51 women and four men) were met inclusion criteria and retrospectively evaluated.

Eighteen hips in 12 patients previously had undergone treatment for developmental dysplasia of the hip (DDH) at the time below 4 years of age. Closed treatment was performed for all 18 hips and successful reduction was obtained in 14 hips. Open reduction was added in the other four hips. CT scans were performed between February 2000 and July 2007. The mean age was 35 years (range 15–64 years). Clinical evaluation was performed according to the Harris hip-scoring system [30].

Pelvic CT scans were acquired at 2.0-mm thickness, and a table speed of 3.0 mm/sec, using a helical scanner (Aquilion, Toshiba, Tokyo, Japan). Helical scanning was conducted at 120 kVp and 300 mAs. The field of view was 380 mm. The patients were placed in supine position, with their hips and knees fully extended, patellae pointing straight up and the feet stabilized in a neutral position.

CT data were transferred digitally to Digital Imaging and Communications in Medicine (DICOM, Rosslyn, VA, USA) format images (512 x 512 pixels) and retrieved using a compact disc or a digital versatile disc. These retrieved data were transferred to a personal laptop computer (VAIO type T, Sony Style Inc, Tokyo, Japan). All 3D image reconstructions were performed on the same personal computer. The 3D bone images of the pelvis and bilateral femur were reconstructed and analyzed using INTAGE Realia and Volume Player software (KGT Inc, Tokyo, Japan). The reconstruction interval on coronal and sagittal images of the hip joint was 0.5-mm. These software allowed easy and free display of 3D pelvic views and cross-sectional images on personal computers. The 3D pelvic images, cross-sectional axial images, cross-sectional sagittal images and cross-sectional coronal images were simultaneously displayed on one field of view (Fig. 1). All CT measurements were performed on the same

laptop computer. Two our consultant radiologists advised us about methods of CT measurements and four orthopaedic surgeons made all measurements.

To calculate the percentage of acetabular coverage of the femoral head, the conventional cranial view was created. We determined the axial plane passing through the top of the bony acetabular roof above the femoral head on the coronal reconstruction image, and then erased part of the ilium which was more cranial than the determined axial plane to create a cranial view. This cranial view indicated the acetabular coverage of the femoral head. We confirmed this view by rotating the view and created posterior, anterior, and lateral views with and without the cross-sectioned pelvis (Fig. 2). Next, the axial plane passing through the center of the femoral head was determined. The ilium and femoral head more cranial than this plane were erased and a cranial view was created. The percentage of acetabular coverage of the femoral head was evaluated by these two cranial views (Fig. 3). These two images were transferred to Image J software (National Institute of Health, Bethesda, MD, USA). Initially, the circumference of the femoral head and the uncovered area were outlined using a non-permanent fine tip marker. The program measures the area of the outlined structure on each particular slice. We calculated the percentage of acetabular coverage of the femoral head as the ratio of coverage area to the whole cross-sectional area of the femoral head. The intraobserver variability for this technique was assessed. Sequential measurements of 84 hips were performed, and other two series of measurements were performed on the other weeks as a blind fashion for previous measurements. These three series of measurements were compared.

The CE angle of Wiberg [6], which is an indication of the lateral coverage of the acetabulum above the femoral head (Fig. 4a), and acetabular index (AI) angle [27], which shows

the lateral tilt or slope of the loading zone of the acetabulum (Fig. 4b), were measured on a reformatted coronal image passing through the center of the femoral head. These two angles were compared with those measured on conventional plain antero-posterior radiographs as a blind fashion. The ACE angle [23], which is an indication of the superior-anterior coverage of the acetabulum, was measured on a reformatted sagittal image passing through the center of the femoral head (Fig. 4c). Acetabular anteversion (AcetAV) angle [25], anterior acetabular sector angle (AASA) [24] and posterior acetabular sector angle (PASA) [24] were measured on a reformatted axial image passing through the centers of the femoral heads (Fig. 4d). The horizontal acetabular sector angle (HASA) [24] was calculated by adding the AASA and PASA. Hips with poor anterior acetabular support were defined as those with an AASA $< 50^\circ$, and hips with poor posterior support were defined as those with a PASA $< 90^\circ$ [25]. According to the AASA and PASA, acetabular dysplasia was classified into four types (Table 1). We categorized hips with mild or global deficiency as having lateral deficiency.

On plain antero-posterior radiographs, we measured the CE angle of Wiberg [6] and acetabular index (AI) angle [27]. These two angles were compared with those measured on reformatted CT coronal images passing through the center of the femoral head as a blind fashion. We observed any cross-over sign of Reynolds et al. [31], which has been reported to be positive retroversion of the acetabulum.

Statistical analyses were performed using SPSS software, version 11.0 (SPSS Inc., Chicago, IL, USA). Mann-Whitney U test, Kruskal-Wallis test and Friedman test were performed. The Pearson linear correlation coefficient (r) was used to assess correlations among various measurements. A probability value less than 0.05 was considered significant.

Results

Twelve hips (14%) were classified as mild deficiency, 22 hips (26%) as anterior deficiency, 17 hips (20%) as posterior deficiency, and 33 hips (39%) as global deficiency (Fig. 5), indicating that 45 hips (54%) had lateral deficiency. The average Harris hip score [30] at the time of 3DCT scans was 82.1 ± 7.5 points (range 64–100 points); 82.4 ± 7.5 points (range 70–100 points) in the anterior deficiency group, 81.8 ± 9.2 points (range 64–94 points) in the posterior deficiency group and 82.0 ± 7.0 points (range 68–100 points) in the lateral deficiency group. No significant difference was found in the hip score among anterior, posterior and lateral deficiency groups (Kruskal-Wallis test, $p = 0.991$).

The analysis of each measurement of the 84 dysplastic hips showed wide variations. Comparisons of CT measurements among various deficiency types are listed in Table 2. In the assessment of various CT measurements among anterior, posterior and lateral deficiency groups, significant differences were found in the ACE angle ($p = 0.001$), AcetAV angle ($p < 0.001$), AASA ($p < 0.001$), PASA ($p < 0.001$) and HASA ($p < 0.001$), and no significant differences were found in the CE angle ($p = 0.261$), AI angle ($p = 0.886$) and the percentage of acetabular coverage ($p = 0.188$). There were significant correlations between acetabular coverage and the CE angle ($r = 0.856$), AI angle ($r = -0.738$), ACE angle ($r = 0.482$), PASA ($r = 0.444$) and HASA ($r = 0.444$). There was no correlation between the AASA and PASA ($r = -0.130$). In 18 hips of 12 patients who had undergone treatment for DDH in childhood, no hip was classified as mild deficiency, four hips as anterior deficiency, three hips as posterior deficiency, and 11 hips as global deficiency. The average acetabular coverage of these 18 hips was 51%,

which was lower than 65% of 66 hips in 44 patients without DDH treatment in childhood (Mann-Whitney U test, $p < 0.001$).

There was a significant correlation between the Harris hip score and the acetabular coverage ($r = 0.523$, $p < 0.001$), indicating that hips with greater acetabular coverage tend to have a higher hip score.

3DCT and conventional plain radiographic measurements were compared in the CE angle and AI angle (Table 3). There was a high correlation between 3DCT and conventional radiographic measurements. Eight of 17 hips with posterior deficiency had the cross-over sign on antero-posterior radiographs.

All 3D image reconstructions could be easily performed on the same personal laptop computer. It took an average of 50 seconds (range 35–95 seconds) to create a 3D image from 2D DICOM formatted images. No failure of 3D reconstruction was found.

Intraobserver variability in measurements of the percentage of acetabular coverage ranged from 0% to 7.8%. Overall average intraobserver differences were 1.4%. No significant difference was found among three series of measurements (Friedman test, $p = 0.177$).

Discussion

This study represents the largest group of adult dysplastic hips without advanced osteoarthritic changes analyzed by 3DCT. Murphy et al. [18] assessed 20 dysplastic hips in 17 women using 3DCT. They did not describe the inclusion criteria of the patients and it was not clear whether patients showing radiographic advanced degenerative changes were included. Anda et al. [25] assessed 33 dysplastic hips in 21 patients. Their study included patients

showing radiographic joint space narrowing and patients who had previously undergone hip surgery. Wiberg [6] found it meaningless to measure the CE angle on grossly abnormal or deformed hips. As osteoarthritis advances, acetabular dysplasia loses its original contour. Although 84 hips in this study were in pre- or early osteoarthritic stage, osteoarthritic changes would likely develop and progress in most of the hips in future as described in previous studies [1, 2, 6, 7]. Our results were obtained from a larger number of patients and will hopefully provide valuable information concerning wide variety of acetabular dysplasia.

Several studies have reported the usefulness of 3D images based on CT data in the assessment of acetabular coverage [10, 11, 15-20, 22, 29]. Klaue et al. [16] overlapped the contours of the femoral head and the acetabulum on multiple conventional CT images before periacetabular osteotomy. Murphy et al. [18] reported the techniques for surface contour reconstruction, measuring lateral, anterior and posterior CE angles to quantify coverage of the femoral head. They emphasized that some patients were deficient globally, some anterolaterally, and some posterolaterally. Azuma et al. [10] studied dysplastic hips before rotational acetabular osteotomy using anterior and posterior views of 3DCT images. Their method was simple and easy, however, they did not employ cranial views which allow direct comparison between anterolateral and posterolateral coverage. Anda [29] suggested that AASA and PASA should be used, rather than anterior and posterior CE angles. Roach et al. [20] reconstructed 3D images before triple innominate osteotomies and assessed the contact area by separating the femoral head from the acetabulum. They concluded that a shelf operation should be performed for patients with severe deficiency in addition to a triple innominate osteotomy. Janzen et al. [15] measured the CE angles in 10° increments around the entire acetabular rim and graphed the average CE

angles obtained from 15 normal hips. Haddad et al. [11] used this technique to achieve the most efficient amount of correction at periacetabular osteotomy and reported that posterior coverage tended to be insufficient when performing periacetabular osteotomy. Nakamura et al. [19] reported that the average acetabular coverage ratio was 65% in a study of 20 dysplastic hips, in which 12 hips (60%) showed radiological degenerative changes and five hips (25%) showed advanced osteoarthritis. Tallroth and Lepistö [22] studied 70 normal hips and described the average values of the CE angle, AI angle, ACE angle, AcetAV angle, AASA and PASA. Mechlenburg et al. [17] measured the projected load-bearing area of the femoral head of six normal hips and six dysplastic hips, and reported that the projected load-bearing area was significantly increased after periacetabular osteotomy.

The measurement of the AcetAV angle, AASA and PASA in the axial plane passing through the centers of the femoral heads has been widely used for the evaluation of hip dysplasia [18, 22, 24, 25, 29]. Normal values for the AcetAV angle were reported to be $19^\circ \pm 4.5^\circ$ [24] (mean and standard deviation) and $17^\circ \pm 6^\circ$ [22] for men, and $22^\circ \pm 5.1^\circ$ [24] and $23^\circ \pm 7^\circ$ [22] and for women. Normal values for the AASA were $64^\circ \pm 6.1^\circ$ [24] and $67^\circ \pm 13^\circ$ [22] for men, and $63^\circ \pm 6.1^\circ$ [24] and $63^\circ \pm 11^\circ$ [22] for women. Normal values for the PASA were $102^\circ \pm 8.4^\circ$ [24] and $103^\circ \pm 11^\circ$ [22] for men, and $105^\circ \pm 7.9^\circ$ [24] and $104^\circ \pm 25^\circ$ [22] for women. These results indicate that the AcetAV angle, AASA and PASA are quite constant and appropriate for evaluation.

In the assessment of dysplastic hips, Murphy et al. [18] reported that values for the AASA were $35^\circ \pm 18^\circ$ and values for the PASA were $80^\circ \pm 7.6^\circ$ in the assessment of 20 hips in 17 women. Anda et al. [25] reported that values for the AASA were $46^\circ \pm 8^\circ$ and values for the

PASA were $92^{\circ} \pm 11^{\circ}$ in the assessment of 33 hips in 21 patients. Although these values are comparable to those in this study (Table 2), our results were obtained from a larger number of patients showing no advanced degeneration, providing valuable information concerning wide variety of acetabular dysplasia.

Statistical analysis showed that each different deficiency type also had various degrees of CE angle and percentages of acetabular coverage. These results indicated that each dysplastic type had various degrees of dysplasia rather than a specific type of severity. The wide variability of obtained measurements suggests that each patient should be considered individually. Deficiency of the acetabulum in patients who had undergone treatment for DDH in childhood was shown to be more severe than those without DDH treatment in childhood.

One mode of failure in periacetabular osteotomy is malpositioning of the acetabular fragment [32]. The osteotomized fragment should be placed appropriately depending on deficiency types and degrees. If the anterior wall of the acetabulum is deficient, the anterior part of the osteotomized fragment should be rotated more laterally than the posterior part of the fragment. Posterolateral shift of the fragment should be performed for patients with posterior deficiency, and lateral shift should be performed for patients with lateral deficiency. The 3DCT facilitates preoperative planning.

The 3D images are easily depicted using recent imaging software [11, 17, 19, 22]. Image data obtained from CT could be transferred digitally to DICOM format images and retrieved by several kinds of electronic media. The retrieved data can be transferred to personal computers, in which 3D images can be easily reconstructed using recent imaging software. These recent improvements facilitate easy evaluation of the severity of acetabular dysplasia. We

should keep in mind, however, that identity theft is a serious problem these days [33], and it is important to protect personal information.

In the assessment of CE angle and AI angle, a high correlation between 3DCT and conventional radiographic measurements was found in this study. To establish the diagnosis of dysplasia, conventional radiograph might be sufficient as previously described [1-9, 23-27]. However, if operative procedures are considered, 3DCT images provide important additional information. Failure to understand an individual patient's dysplasia will result in an inappropriate operation [10, 32].

Early joint-preserving surgical treatment was reported to prevent or defer the natural history of osteoarthritis in patients with hip dysplasia [34]. Periacetabular osteotomy, Chiari pelvic osteotomy and shelf procedure are options. Stulberg and Harris [3] reported that the average CE angle of Wiberg [6] of 60 normal patients was 37° (range 26°–48°) in men and 35° (range 24°–46°) in women. Murphy et al. [2] reported that the average CE angle of 46 hips in patients who survived to 65 years without osteoarthritis was 34° (range 16°–49°). A postoperative CE angle of approximately 35° seems to be an appropriate goal for correction considering these results.

The CT-based studies have the obvious disadvantage of radiation exposure to the patient, high cost and limited accessibility. However, the development of 3DCT techniques facilitated assessments and understanding of dysplastic anatomy. As each acetabular deficiency type has varying degrees of dysplasia, 3DCT is useful to precisely analyze individual characteristics.

In conclusion, our results were obtained from a larger number of patients and might

provide valuable information concerning wide variety of deficiency type and degree of acetabular dysplasia. Hips with greater acetabular coverage tended to have a higher Harris hip score.

Preoperative evaluation using 3DCT scans should be considered to understand the deficiency type and degree of acetabular dysplasia.

Captions of figures

Fig. 1 Four images are simultaneously displayed on one field of view. (a) Three-dimensional pelvic image is displayed on the left upper part of the view. Cross-cursor is used to seek the exact center of the femoral head among the (b) axial, (c) sagittal, and (d) coronal images.

Fig. 2 We decide the axial plane passing through the top of the bony acetabular roof above the femoral head on the coronal view, and then create cranial view in which a more cranial part of the ilium than the decided axial plane was erased (a). This cranial view indicates acetabular coverage of the femoral head. We confirm this cranial view by rotating the view and creates (b) postero-cranial, (c) posterior, (d) anterior, and (e, f) lateral views with and without cross-sectioned pelvis.

Fig. 3 The circumference of the femoral head and the uncovered area were outlined using a non-permanent fine tip marker. The percentage of acetabular coverage of the femoral head was calculated as the ratio of the coverage area to the whole cross-sectional area of the femoral head.

a Uncovered area of the femoral head is outlined.

b Whole femoral head on the axial image passing through the center of the femoral head is outlined.

Fig. 4 a The center-edge (CE) angle of Wiberg [6] is measured on a reformatted coronal image passing through the center of the femoral head. The CE angle represents the angle between the vertical axis of the pelvis and a line running through the center point and the lateral acetabular margin.

b The acetabular index angle [27] (AI angle, lateral tilt of the acetabulum) is measured on a

reformatted coronal image passing through the center of the femoral head. The AI angle represents the angle between the pelvic horizontal line and the line through the lateral margin of the acetabulum and the superior edge of the fovea.

c Anterior center-edge (ACE) angle [23] is measured on a reformatted sagittal image passing through the center of the femoral head. The ACE angle represents the angle between the horizontal line and the line through the most superior point of the acetabular joint surface and anterior margin of the acetabulum.

d Acetabular anteversion (AcetAV) angle [25], anterior acetabular sector angle (AASA) [24] and posterior acetabular sector angle (PASA) [24] are measured on a reformatted axial image passing through the center of the femoral head. The AcetAV angle is the angle between the line combining the anterior and posterior margins of the acetabulum and the line perpendicular to the centerline combining the bilateral femoral heads. AASA and PASA are the angles between the centerline combining the bilateral femoral heads and lines from the center of the head to the anterior and posterior margins of the acetabulum.

Fig. 5 Cross-sectional cranial views show anterior, posterior, and global deficiency.

a Cross-sectional cranial view of a 21-year-old woman shows anterior deficiency.

b Cross-sectional cranial view of a 39-year-old woman shows posterior deficiency. The shape of the pelvis looks different from those of **a** and **c**, suggesting different growth direction or pattern of the pelvic bone.

c Cross-sectional cranial view of a 28-year-old woman shows global deficiency.

References

1. Malvitz TA, Weinstein SL. Closed reduction for congenital dysplasia of the hip: functional and radiographic results after an average of thirty years. *J Bone Joint Surg Am* 1994; 76: 1777-1792.
2. Murphy SB, Ganz R, Müller ME. The prognosis in untreated dysplasia of the hip: a study of radiographic factors that predict the outcome. *J Bone Joint Surg Am* 1995; 77: 985-989.
3. Stulberg SD, Harris WH. Acetabular dysplasia and development of osteoarthritis of the hip. *The Hip. Proceedings of the Second Open Scientific Meeting of The Hip Society. St Louis: CV Mosby, 1974: 82-93.*
4. Wedge JH, Wasylenko MJ. The natural history of congenital dislocation of the hip: a critical review. *Clin Orthop Relat Res* 1978; 137: 154-162.
5. Wedge JH, Wasylenko MJ. The natural history of congenital disease of the hip. *J Bone Joint Surg Br* 1979; 61: 334-338.
6. Wiberg G. Studies on dysplastic acetabula and congenital subluxation of the hip joint: with special reference to the complication of osteoarthritis. *Acta Chir Scand* 1939; 83(Suppl 58): 1-135.
7. Wiberg G. Shelf operation in congenital dysplasia of the acetabulum and in subluxation and dislocation of the hip. *J Bone Joint Surg Am* 1953; 35: 65-80.
8. Hadley NA, Brown TD, Weinstein SL. The effects of contact pressure elevations and aseptic necrosis on the long-term outcome of congenital hip dislocation. *J Orthop Res* 1990; 8: 504-513.

9. Maxian TA, Brown TD, Weinstein SL. Chronic stress tolerance levels for human articular cartilage: two nonuniform contact models applied to long-term follow-up of CDH. *J Biomech* 1995; 28: 159-166.
10. Azuma H, Taneda H, Igarashi H, Fujioka M. Preoperative and postoperative assessment of rotational acetabular osteotomy for dysplastic hips in children by three-dimensional surface reconstruction computed tomography imaging. *J Pediatr Orthop* 1990; 10: 33-38.
11. Haddad FS, Garbuz DS, Duncan CP, Janzen DL, Munk PL. CT evaluation of periacetabular osteotomies. *J Bone Joint Surg Br* 2000; 82: 526-531.
12. Hernandez RJ. Concentric reduction of the dislocated hip: computed-tomographic evaluation. *Radiology* 1984; 150: 266-268.
13. Hubbard AM, Dormans JP. Evaluation of developmental dysplasia, Perthes disease, and neuromuscular dysplasia of the hip in children before and after surgery: an imaging update. *AJR Am J Roentgenol* 1995; 164: 1067-1073.
14. Jacobsen S, Rømer L, Søballe K. Degeneration in dysplastic hips: a computer tomography study. *Skeletal Radiol* 2005; 34: 778-784.
15. Janzen D, Aipperesbach SE, Munk PL, et al. Three-dimensional CT measurement of adult acetabular dysplasia: technique, preliminary results in normal subjects and potential applications. *Skeletal Radiol* 1998; 27: 352-358.
16. Klaue K, Wallin A, Ganz R. CT evaluation of coverage and congruency of the hip prior to osteotomy. *Clin Orthop Relat Res* 1988; 232: 15-25.

17. Mechlenburg I, Nyengaard JR, Rømer L, Søballe K. Changes in load-bearing area after Ganz periacetabular osteotomy evaluated by multislice CT scanning and stereology. *Acta Orthop Scand* 2004; 75: 147-153.
18. Murphy SB, Kijewski PK, Millis MB, Harless A. Acetabular dysplasia in the adolescent and young adult. *Clin Orthop Relat Res* 1990; 261: 214-223.
19. Nakamura S, Yorikawa J, Otsuka K, Takeshita K, Harasawa A, Matsushita T. Evaluation of acetabular dysplasia using a top view of the hip on three-dimensional CT. *J Orthop Sci* 2000; 5: 533-539.
20. Roach JW, Hobatho MC, Baker KJ, Ashman RB. Three-dimensional computer analysis of complex acetabular insufficiency. *J Pediatr Orthop* 1997; 17: 158-164.
21. Schlesinger AE, Hernandez RJ. Diseases of the musculoskeletal system in children: imaging with CT, sonography, and MR. *AJR Am J Roentgenol* 1992; 158: 729-741.
22. Tallroth K, Lepistö J. Computed tomography measurement of acetabular dimensions: normal values for correction of dysplasia. *Acta Orthop Scand* 2006; 77: 598-602.
23. Lequesne M, de Sèze S. Le faux profil du bassin: nouvelle incidence radiographique pour l'étude de la hanche: son utilité dans les dysplasies et les différentes coxopathies. *Rev Rhum* 1961; 28: 643-652.
24. Anda S, Svenningsen S, Dale LG, Benum P. The acetabular sector angle of the adult hip determined by computed tomography. *Acta Radiol Diagn* 1986; 27: 443-447.
25. Anda S, Terjesen T, Kvistad KA, Svenningsen, S. Acetabular angles and femoral anteversion in dysplastic hips in adults: CT investigation. *J Comput Assist Tomogr* 1991; 15: 115-120.

26. Crowe JF, Mani VJ, Ranawat CS. Total hip replacement in congenital dislocation and dysplasia of the hip. *J Bone Joint Surg Am* 1979; 61: 15-23.
27. Tönnis D. Congenital dysplasia and dislocation of the hip in children and adults. Berlin, etc: Springer-Verlag, 1987.
28. Tönnis D, Heinecke A. Acetabular and femoral anteversion: relationship with osteoarthritis of the hip. *J Bone Joint Surg Am* 1999; 81: 1747-1770.
29. Anda S. Letter to Editor. *Clin Orthop Relat Res* 1993; 286: 308-310.
30. Harris WH. Traumatic arthritis of the hip after dislocation and acetabular fractures: treatment by mold arthroplasty: an end-result study using a new method of result evaluation. *J Bone Joint Surg Am* 1969; 51: 737-755.
31. Reynolds D, Lucas J, Klaue K. Retroversion of the acetabulum: a cause of hip pain. *J Bone Joint Surg Br* 1999; 81: 281-288.
32. Trousdale RT, Cabanela ME. Lessons learned after more than 250 periacetabular osteotomies. *Acta Orthop Scand* 2003; 74: 119-126.
33. Deapen D. Cancer surveillance and information: balancing public health with privacy and confidentiality concerns (United States). *Cancer Causes Control* 2006; 17: 633-637.
34. Søballe K. Hip dysplasia. Treatment with osteotomy by means of Ganz: The Danish Orthopedic Society. *Ugeskr Laeger* 2001; 163(12): 1703.

Table 1 Classification of acetabular dysplasia

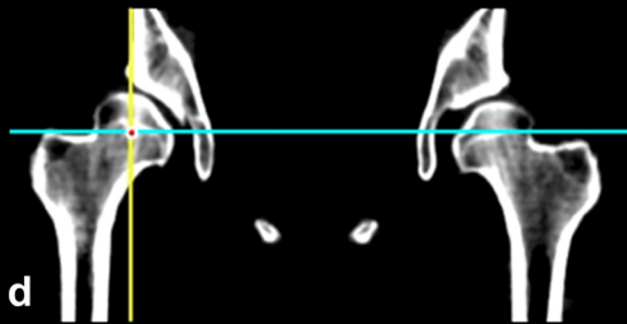
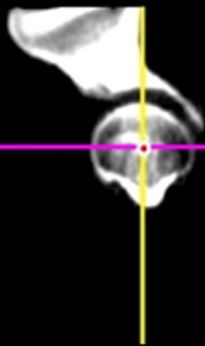
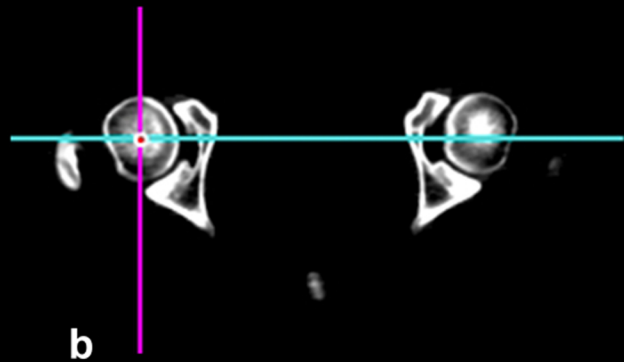
	Mild deficiency	Anterior deficiency	Posterior deficiency	Global deficiency
Anterior acetabular sector angle (AASA) [24]	$\geq 50^\circ$	$< 50^\circ$	$\geq 50^\circ$	$< 50^\circ$
Posterior acetabula sector angle (PASA) [24]	$\geq 90^\circ$	$\geq 90^\circ$	$< 90^\circ$	$< 90^\circ$

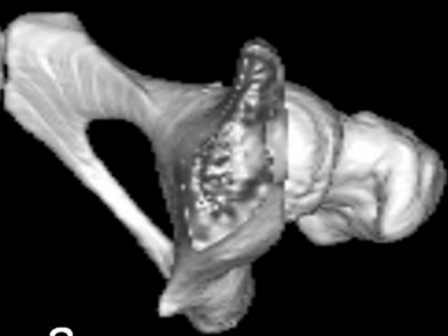
Table 2 Comparison of CT measurements among various deficiency types. The values are given as the mean and standard deviation.

	Mild deficiency (n = 12)	Anterior deficiency (n = 22)	Posterior deficiency (n = 17)	Global deficiency (n = 33)	Lateral deficiency (= Mild + Global deficiency, n = 45)	Total (n = 84)
Center-edge (CE) angle [6] (°)	14.7 ± 4.1	11.4 ± 6.5	9.8 ± 5.7	6.3 ± 7.7	8.5 ± 7.9	9.5 ± 7.2
Acetabular index (AI) angle [27] (°)	16.7 ± 8.2	20.6 ± 7.1	20.8 ± 8.0	23.4 ± 8.9	21.6 ± 9.1	21.2 ± 8.3
Anterior center-edge (ACE) angle [23] (°)	19.7 ± 5.7	17.0 ± 7.9	22.9 ± 5.7	8.6 ± 15.1	11.6 ± 14.1	15.3 ± 12.2
Acetabular anteversion (AcetAV) angle [25] (°)	19.1 ± 4.9	27.5 ± 3.5	14.4 ± 8.0	20.2 ± 3.6	19.9 ± 4.0	20.8 ± 6.7
Anterior acetabular sector angle (AASA) [24] (°)	55.2 ± 5.1	40.7 ± 5.1	55.8 ± 7.9	41.7 ± 6.2	45.3 ± 8.4	46.2 ± 9.1
Posterior acetabular sector angle (PASA) [24] (°)	92.4 ± 3.9	94.8 ± 4.3	81.9 ± 4.9	82.3 ± 3.7	85.0 ± 5.9	86.9 ± 7.2
Horizontal acetabular sector angle (HASA) [24] (°)	147.6 ± 5.3	135.6 ± 7.7	137.7 ± 6.2	124.0 ± 7.6	130.3 ± 12.7	133.2 ± 10.9
Acetabular coverage (%)	65.7 ± 7.3	65.6 ± 6.1	62.0 ± 8.5	58.6 ± 11.0	60.5 ± 10.6	62.1 ± 9.3

Table 3 Comparison of center-edge angle and acetabular index angle on 3DCT and plain radiograph (*SD* standard deviation)

	CT			X-p			r
	Mean	Range	SD	Mean	Range	SD	
Center-edge (CE) angle [6] (°)	9.5	-15 – 19	7.2	9.9	-14 – 19	6.7	0.999
Acetabular index (AI) angle [27] (°)	21.2	4 – 40	8.3	20.3	3 – 38	8.3	0.993





a



b



c



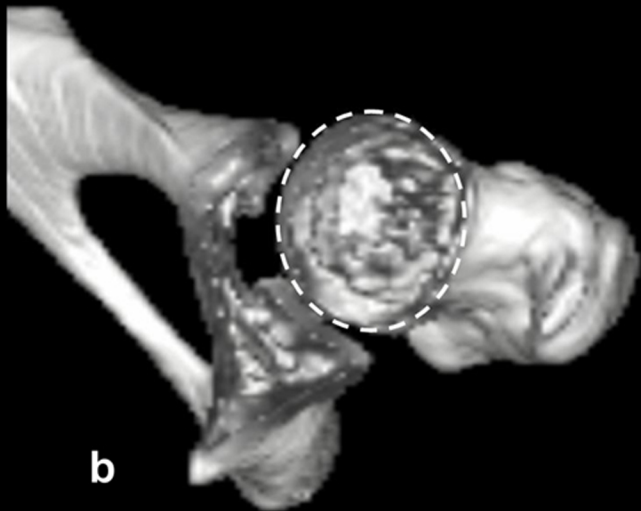
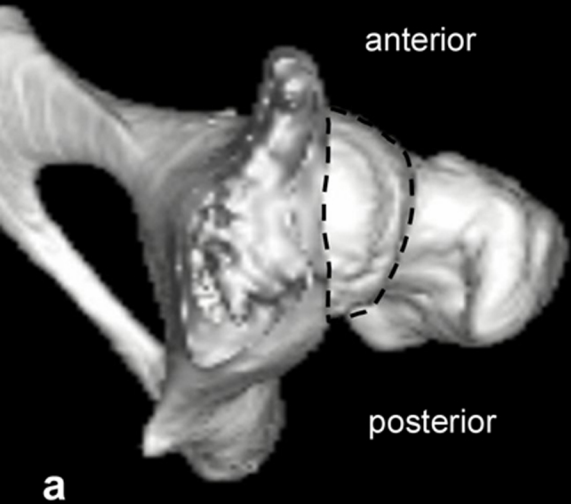
d



e



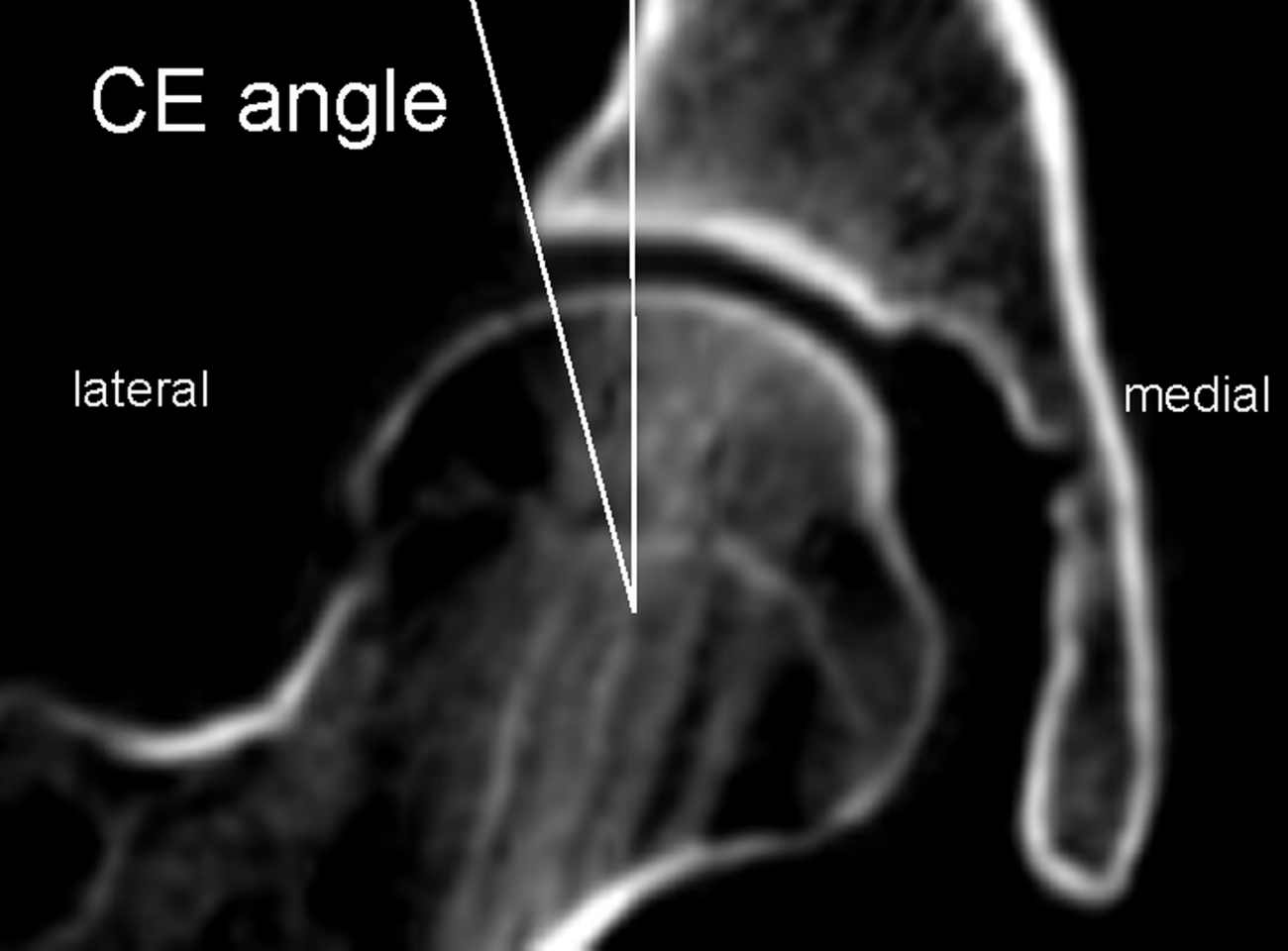
f



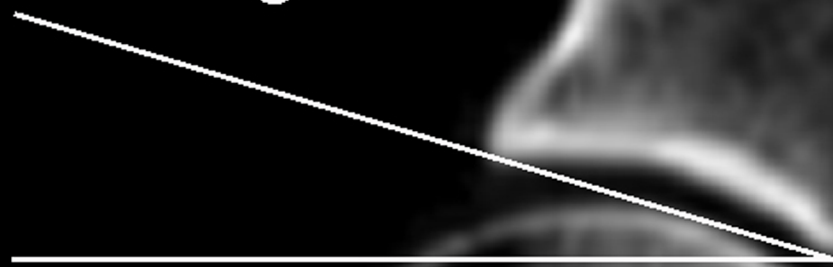
CE angle

lateral

medial

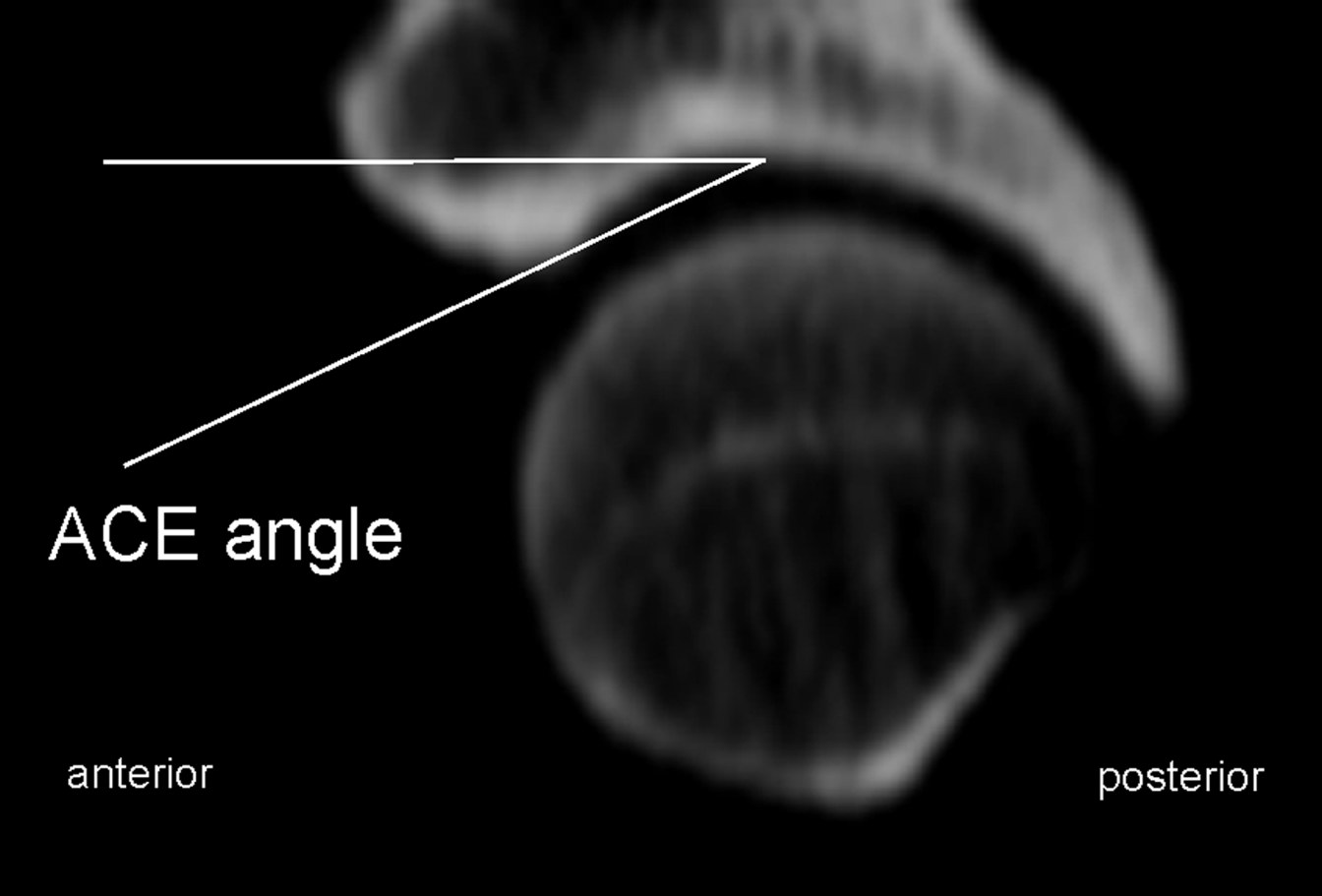


AI angle



lateral

medial



ACE angle

The image shows a grayscale cross-section of a vertebral body. A horizontal white line is drawn from the left edge to the anterior margin of the vertebral body. A second white line is drawn from the same point on the horizontal line to the superior margin of the vertebral body. The angle between these two lines is labeled 'ACE angle'. The vertebral body is roughly circular with a textured internal structure. The superior margin is slightly curved. The background is black.

anterior

posterior

